ELSEVIER

Improved biological performance of Ti implants due to surface modification by micro-arc oxidation

Long-Hao Li[a], Young-Min Kong[a], Hae-Won Kim[a], Young-Woon Kim[a], Hyoun-Ee Kim[a],*, Seong-Joo Heo[b], Jai-Young Koak[b]

[a] *School of Materials Science and Engineering, Seoul National University, Seoul, 151-742, South Korea*
[b] *Department of Prosthodontics, College of Dentistry, Seoul National University, Seoul, South Korea*

Abstract

The surface of a titanium (Ti) implant was modified by micro-arc oxidation (MAO) treatment. A porous layer was formed on the Ti surface after the oxidation treatment. The phase and morphology of the oxide layer were dependent on the voltage applied during the oxidation treatment. With increasing voltage, the roughness and thickness of the film increased and the TiO_2 phase changed from anatase to rutile. During the MAO treatment, Ca and P ions were incorporated into the oxide layer. The in vitro cell responses of the specimen were also dependant on the oxidation conditions. With increasing voltage, the ALP activity increased, while the cell proliferation rate decreased. Preliminary in vivo tests of the MAO-treated specimens on rabbits showed a considerable improvement in their osseointegration capability as compared to the pure titanium implant.
© 2003 Elsevier Ltd. All rights reserved.

Keywords: Titanium; Oxidation; Biocompatibility; In vitro; Osseointegration; In vivo

1. Introduction

Pure titanium (Ti) and titanium alloys are frequently used as dental and orthopedic implant materials because of their excellent mechanical strength, chemical stability, and biocompatibility [1]. The biocompatibility of titanium is closely related to the properties of the surface oxide layer, in terms of its structure, morphology and composition. Various physical and chemical treatments of the Ti surface have been proposed with a view to obtaining the most biocompatible implant surface. Among the techniques, which have been found to be beneficial to the biological performance of the implants, are increasing the surface roughness, the oxidation of Ti to form a TiO_2 layer on the surface. The incorporation of Ca or P ions into the surface layer, and the validity of these results has been confirmed by several different researchers [2–5]. The most widely used commercial techniques are sandblasting, acid-etching, and the plasma spraying of hydroxyapatite [6,7].

Recently, an electrochemical procedure for modifying the Ti surface was proposed, which has since attracted much attention. By applying a positive voltage to a Ti specimen immersed in an electrolyte, anodic oxidation (or anodizing) of Ti occurs to form a TiO_2 layer on the surface. When the applied voltage is increased to a certain point, a micro-arc occurs as a result of the dielectric breakdown of the TiO_2 layer. At the moment that the dielectric breakdown occurs, Ti ions in the implant and OH ions in the electrolyte move in opposite directions very quickly to form TiO_2 again. This process is generally referred to as micro-arc oxidation (MAO) or plasma electrolysis [8]. The newly formed TiO_2 layer is both porous and firmly adhered to the substrate, which is beneficial for the biological performance of the implants. Another advantage of this MAO process is the possibility of incorporating Ca and P ions into the surface layer, by controlling the composition and concentration of the electrolyte [9,10]. The incorporated Ca and P ions were even crystallized into hydroxyapatite or other calcium phosphates by a hydrothermal treatment [10,11]. Recent studies on the biological response of Ti implants demonstrated that the MAO process constitutes one of the best methods of modifying the

---

*Corresponding author. Tel.: +82-2-880-7161; fax: +82-02-884-1413.

E-mail address: kimhe@snu.ac.kr (H.-E. Kim).

implant surface [12–17]. However, further research is necessary for the complete characterization of the oxide layer and also for the identification of the optimum conditions for the MAO process.

In this study, we formed TiO_2 layers with different thicknesses and roughnesses on the Ti surface, by controlling the applied voltage used in the MAO process. The phase, composition and morphology of the oxide layer were monitored with respect to the applied voltage. The biological properties of the layers were evaluated by in vitro tests, in terms of the proliferation and differentiation of certain cell lines. Preliminary in vivo tests were also carried out to confirm the results obtained during the in vitro tests.

2. Materials and methods

2.1. Micro-arc oxidation (MAO)

Commercially available pure Ti (CP-Ti, Grade 2, Ka-Hee Metal Industry Co., Seoul, Korea), machined into disks with dimensions of 12 mm (diameter) × 1 mm (thickness), was used as the substrate. These disks were ground using 400-grit SiC sandpaper and cleaned ultrasonically in acetone, ethanol and de-ionized water. MAO of the specimen was carried out in an aqueous electrolyte, by applying a pulsed DC field to the specimen. The frequency and duty of the pulsed DC power were 660 Hz and 10%, respectively. The electrolyte was prepared by dissolving 0.15 mol calcium acetate monohydrate $\{Ca(CH_3COO)_2 \cdot H_2O\}$ and 0.02 mol calcium glycerophosphate $(CaC_3H_7O_6P)$ in de-ionized water. To obtain oxide layers with different degrees of roughness and thickness, a wide range of DC fields (190–600 V) were applied to the specimens, with each treatment lasting 3 min. All of the MAO processing was carried out in a water-cooled bath made of stainless steel, and a stainless steel plate $(100 \times 60 \times 1 \, mm^3)$ was used as the counter electrode.

2.2. Characterization of oxide layer

The phase and microstructure of the specimens were evaluated by X-ray diffraction (XRD; M18XHF-SRA, MacScience Co., Yokohama, Japan) analysis and scanning electron microscopy (SEM; JSM-5600, JEOL, Tokyo, Japan), respectively. The composition of the surface layer was analyzed with an energy dispersive spectroscope (EDS) incorporated into the scanning electron microscope. The structure of the oxidized layer was examined by using a cross-sectional transmission electron microscope (XTEM; JEM-3000F, TEMJEOL, Tokyo, Japan) at an acceleration voltage of 300 kV. The surface roughness was measured by means of an optical interferometer (Accura 2000®, Intekplus Co., Seoul,

Korea). Two parameters, the average roughness (R_a) and 10 point average roughness (R_z), were used to characterize the roughness of the specimens.

2.3. Biological properties

The biological properties of the specimens were evaluated by in vitro cell tests and preliminary in vivo tests. For the in vitro tests, the MG63 and human osteosarcoma (HOS) cell lines were used to characterize the proliferation and differentiation behaviors of the cells, respectively. The pre-incubated cell lines were plated onto specimens with a cell density of $1.5 \times 10^4 \, cells/cm^2$ for the MG63 cells and $5 \times 10^3 \, cells/cm^2$ for the HOS cells, and then cultured in a humidified incubator with 5% CO_2 at 37°C. Dulbecco's modified Eagle's medium (DMEM, Life Technologies, Inc., USA) supplemented with 10% fetal bovine serum (FBS, Life Technologies, Inc., USA) was used as the culturing medium.

The proliferation behavior was determined by counting the number of cells after culturing them for 7 days. The cells were detached from the specimens with 0.05% trypsin-EDTA and counted using a hemocytometer (Superior Co., Germany). The differentiation behavior was estimated by measuring the alkaline phosphatase (ALP) activity of the HOS cells after culturing them for 10 days [18]. The cell layers were washed with Hank's balanced salt solution (HBSS) and detached using trypsin-EDTA solution. After centrifugation at 1200 rpm for 7 min, the cell pellets were washed once with PBS and resuspended by vortexing them in 200 μl of 0.1% Triton X-100. The pellets were disrupted by four cycles of successive freezing and thawing. After centrifugation, the cell lysates were assayed colorimetrically in order to measure their ALP activity using p-nitrophenyl phosphate as the substrate (Sigma, St. Louis, MO, USA). The reaction lasted for 60 min at 37°C, and was then stopped by quenching on ice. The quantity of p-nitrophenol produced was measured at 410 nm using a spectrophotometer (Shimadzu, Japan). The morphology of the proliferated cells was observed by means of SEM after fixation with 2.5% glutaraldehyde, dehydration with graded ethanols (70%, 90% and 100%), and critical point drying using CO_2. Each set of tests was performed in triplicate, and the data was normalized by taking the surface area into consideration.

The in vivo tests were carried out using screw-shaped Ti implants with dimensions of 4.0 mm in length and 3.75 mm in outer diameter and with a pitch-height of 0.5 mm. The implants were treated by means of the MAO process at a voltage of 270 V. For the purpose of comparison, as-machined implants were also tested. Ten female, New Zealand white rabbits, weighing 3–3.5 kg and aged from 9 to 10 months, were used for the tests.

After general anesthesia, four implants were placed into each rabbit, two in each proximal tibial metaphysis. The holes for the implantation were drilled using a low-speed rotary instrument with profuse saline irrigation. The diameter of the drill was successively increased, and the insertion sites were finalized with a 3.75 mm tap without countersinking [19]. After a healing period of 4 weeks, the rabbits were sacrificed and, in each case, the bond strength between the bone and the implant was measured with a torque measurement device (Shinsung Co., Seoul, Korea). After the removal torque tests, the morphology of each implant was observed by means of SEM.

3. Results

3.1. Morphology of oxide layer

The surface morphologies of the Ti after MAO using different treatment conditions are shown in Figs. 1(A)–(F). Before the oxidation treatment, only the machining grooves were observed on the surface. When a pulsed DC field of 190 V was applied, a porous oxide layer began to be formed, as shown in Fig. 1(A). When the field was lower than 190 V, this layer was very thin and uniform without any porosity. As the voltage increased to 230 V, the whole layer became porous as shown in Fig. 1(B), but was not yet uniform throughout the surface. After further increasing the voltage to 270 V, the layer became uniformly porous (Fig. 1(C)). The resulting layer was actually composed of small craters with holes at the center. When the voltage was increased to 350 V, the size of these craters became so large that they were connected together, as shown in Fig. 1(D), and the presence of tiny cracks was observed. When the voltage attained 450 V, the size of the holes, as well as that of the craters, became much larger (Fig. 1(E)), and this trend continued as the applied voltage was further increased up to 600 V (Fig. 1(F)).

The cross-sections of the oxide layers produced by different applied voltages are shown in Figs. 2(A)–(C). At voltages of 190 V or lower, the oxide layer was scarcely observable. When the voltage attained 230 V,
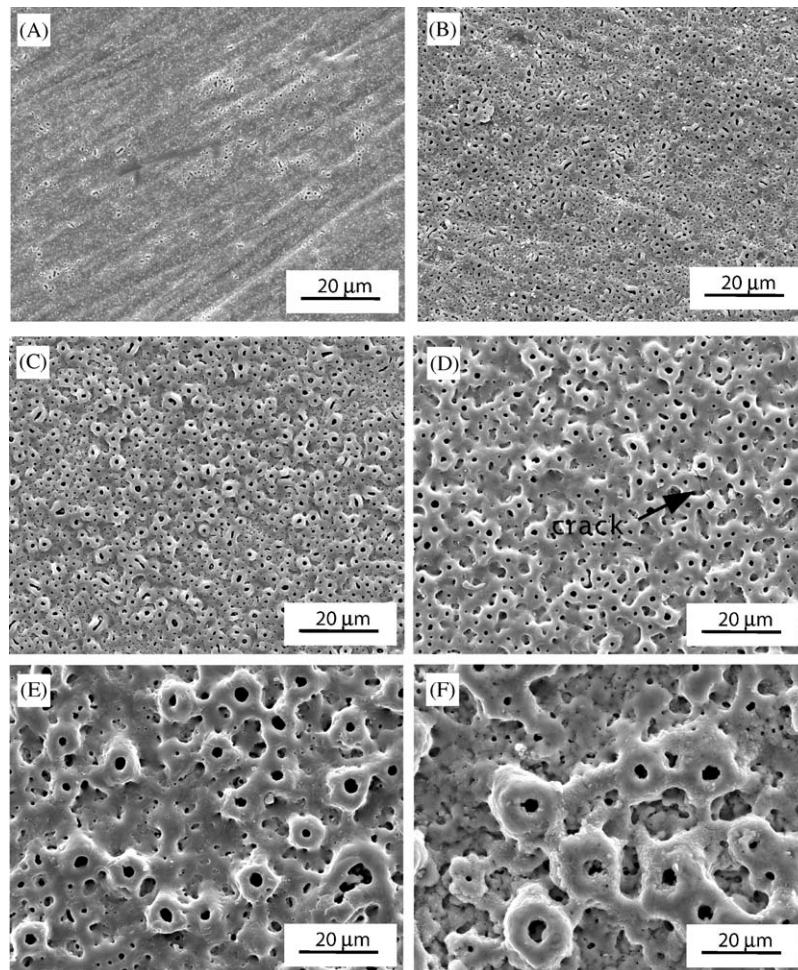

Fig. 1. SEM surface morphologies of Ti surfaces treated with MAO at different voltages: (A) 190 V, (B) 230 V, (C) 270 V, (D) 350 V, (E) 450 V and (F) 600 V. (The arrow in (D) indicates the crack formed on the layer).
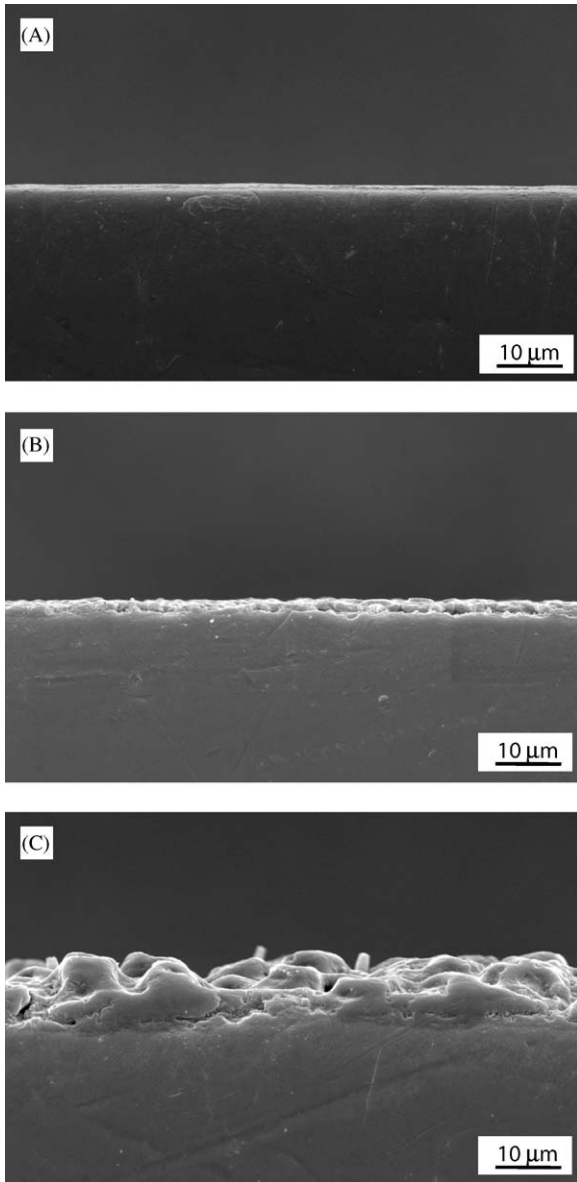
Fig. 2. SEM cross-sectional views of Ti specimens treated with MAO at different voltages: (A) 230 V, (B) 270 V and (C) 450 V.

Fig. 3. Thickness of oxide layer as a function of the applied voltage. Error bars stand for ± 1 standard deviations.

Fig. 4. Roughness of the oxide layer as a function of the applied voltage: R_a, average roughness and R_z, 10 point average roughness. Error bars stand for ± 1 standard deviations.

the oxide layer was clearly visible, as shown in Fig. 2(A). With increasing voltage, the layer became thicker, as shown in Fig. 2(B), which corresponds to the layer formed at 270 V. Above 270 V, thickness of the layer continued to increase with increasing voltage. The layer formed at 450 V, which can be seen in Fig. 2(C), clearly shows the rough and porous nature of the oxide layer produced in this case.

Using these cross-sectional micrographs, the thickness of the layer was measured as a function of the applied voltage. As expected, the thickness was almost linearly dependent on the voltage, as shown in Fig. 3.

The roughness of the oxide layer was characterized by two parameters, the average roughness (R_a) and the 10 point average 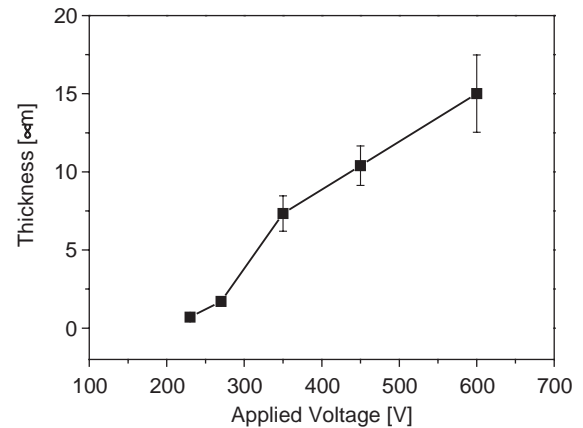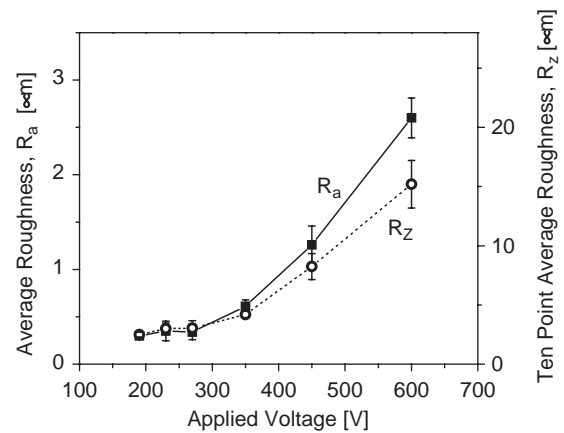roughness (R_z). As the applied voltage increased, the values of both R_a and R_z increased slowly at low voltages, however, above 300 V, they increased rapidly as shown in Fig. 4.

3.2. Phase and structure

The phase of the oxide layers formed by the MAO process was characterized by XRD analysis, as shown in Figs. 5(A)–(F). At the relatively low voltage of 190 V, TiO_2 of anatase phase began to form, Fig. 5(A). With increasing voltage, the intensity of the anatase TiO_2 peaks increased until 270 V, as shown in Figs. 5(B)–(C). However, above 270 V, rutile phase, in addition to anatase, began to be detected, as shown in Fig. 5(D). After further increasing the voltage, the intensity of the rutile phase increased, while that of anatase decreased steadily, as shown in Figs. 5(E)–(F).

The chemical composition of the surface layer formed by the MAO process was determined by EDS analysis, as shown in Fig. 6. The concentrations of Ca, P and O
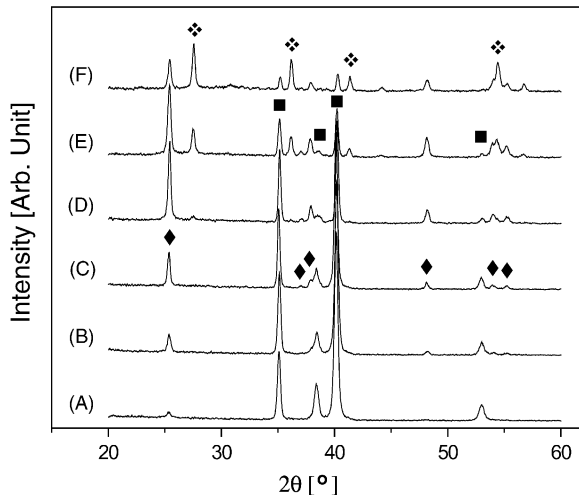
Fig. 5. XRD patterns of Ti substrates after MAO at (A) 190 V, (B) 230 V, (C) 270 V, (D) 350 V, (E) 450 V and (F) 600 V. (■), Ti; (♦), anatase TiO_2 (❖), rutile TiO_2.
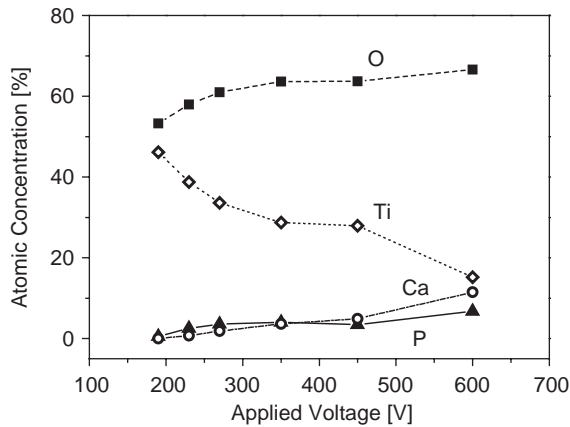

Fig. 6. Chemical composition of the surface layer as a function of the MAO voltage.

Fig. 7. Cross-sectional TEM image and electron diffraction pattern of the MAO-treated Ti at 190 V.

increased with increasing MAO voltage, while that of Ti decreased steadily.

The TiO_2 layer was closely observed with the cross-sectional TEM (XTEM), and a typical microstructure of the oxide layer is shown in Fig. 7. This micrograph shows that there are some internal voids present in the TiO_2 layer. An electron diffraction pattern, in the inset, indicates that the layer which was oxidized at 190 V was composed of anatase phase, confirming the results of the XRD analyses.

3.3. Biocompatibility

The morphologies of the MG63 cells grown on the specimens for 3 days are shown in Fig. 8. On pure Ti, the cells were in close contact with the specimen and spread out uniformly over the surface, as shown in Fig. 8(A). The morphologies of the cells grown on the MAO-
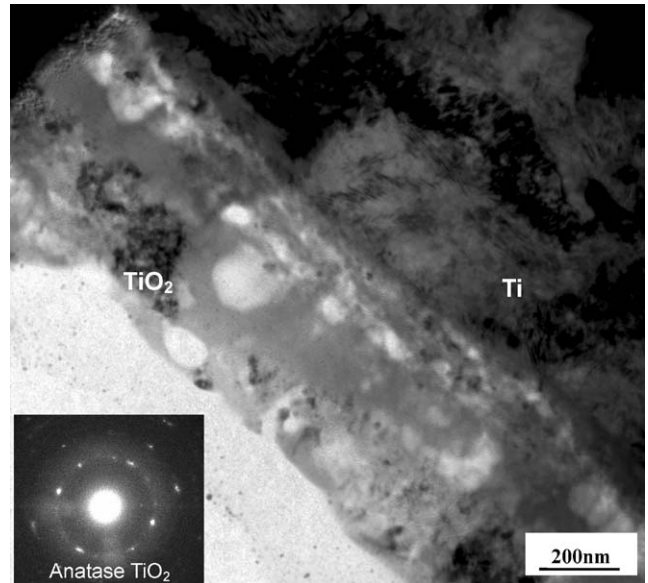
treated specimens were not much different when the applied voltage was relatively low, as illustrated in Fig. 8(B). However, when the applied voltage was excessively high (> 300 V), the number of cells decreased, as shown in Fig. 8(C).

The number of cells was counted after culturing them for 7 days. In all cases, the cells proliferated at least 10 times compared to the originally plated cells. When the Ti was MAO treated at 190 V, the proliferation rate was the highest. As the voltage used for the oxidation process increased, the number of cells decreased steadily, as shown in Fig. 9.

The differentiation behavior of the cells was quite different from the proliferation behavior. The ALP activities of the HOS cells cultured for 10 days on various specimens are shown in Fig. 10. The ALP activity was not much affected by the MAO process when the applied voltage was lower than 300 V. However, when the voltage was higher than 300 V, the activity of the cells increased rapidly, as shown in Fig. 10.

Along with the in vitro cell tests, preliminary in vivo experiments were performed by measuring the removal torque of the specimens implanted in the tibia of the rabbits. The removal torques of the MAO treated at 270 V and the as-machined Ti implants after a 4 weeks healing period are presented in Table 1. Without the MAO treatment, the average removal torque was 12.6 ± 5 N cm. When the implants were MAO treated using an applied voltage of 270 V, the average removal torque values increased markedly to 43.2 ± 12 N cm. After the removal torque tests, the implant surfaces were observed by means of SEM. Small chips adhered to the
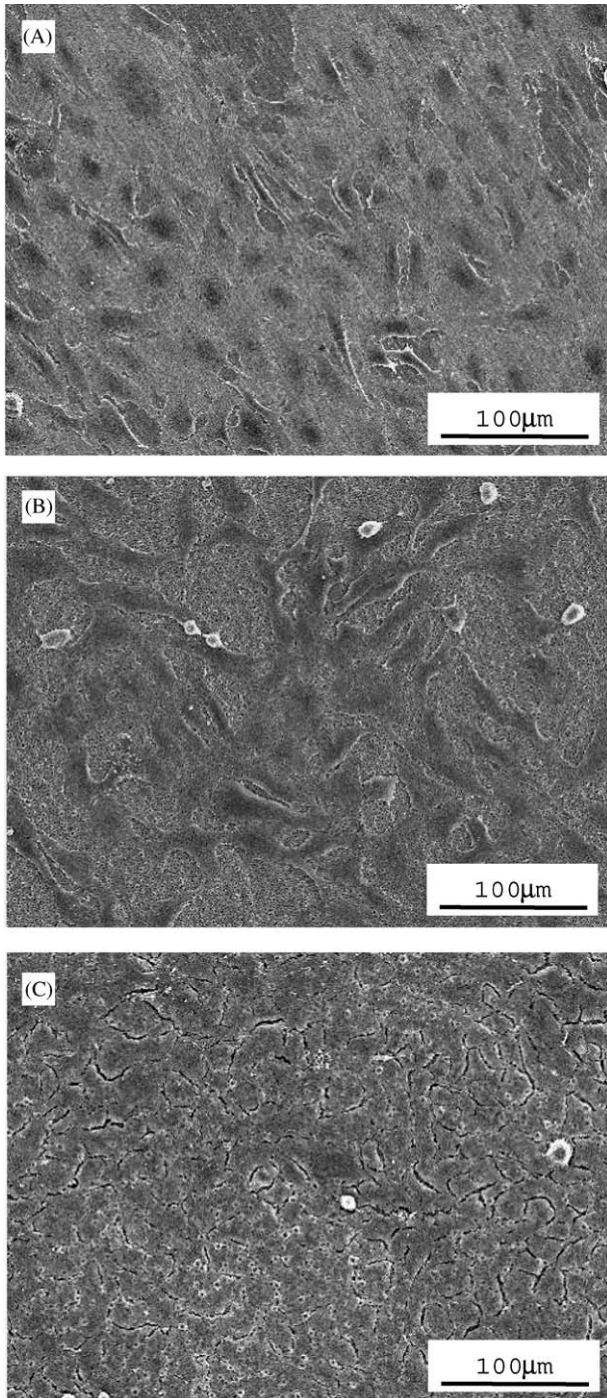
Fig. 8. SEM morphology of MG63 cells after culturing for 3 days on (A) pure Ti, and MAO-treated Ti at (B) 270 V and (C) 350 V.

Fig. 9. Number of MG63 cells after proliferation for 7 days. Each set of tests was performed in triplicate and error bars stand for ± 1 standard deviations.

Fig. 10. ALP activity of HOS cells cultured for 10 days. Each set of tests was performed in triplicate and error bars stand for ± 1 standard deviations.

implant surface were observed, as shown in Figs. 11(A)–(B). From the EDS analyses, these chips were found to possess high concentrations of Ca and P, confirming them to be connective tissues. A greater number of adhered chips were detected in the case of the MAO treated specimens than in the case of the pure Ti ones.
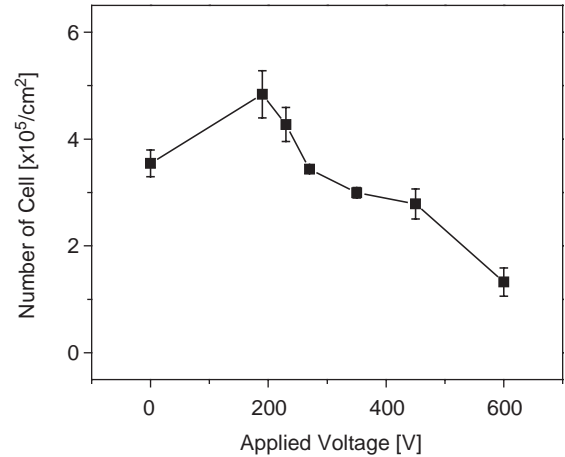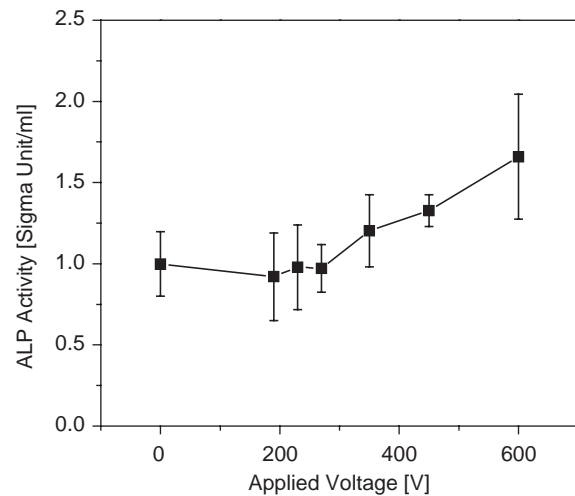
Table 1
Removal torque after 4 weeks (Unit: N cm)

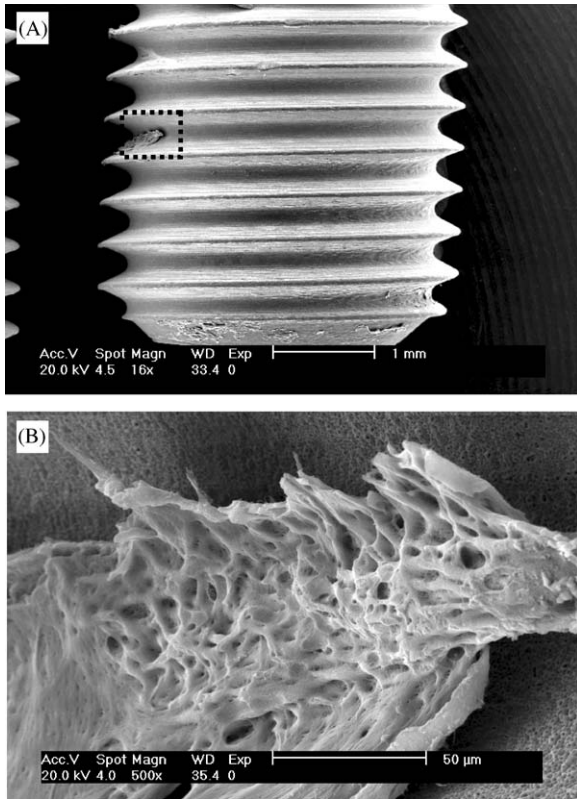| Specimen No.	As-machined pure Ti	Micro-arc oxidized Ti
1	10	32
2	24	62
3	8	30
4	8	62
5	18	32
6	14	46
7	12	50
8	10	44
9	10	32
10	12	42
Average ± 1 SD	12.6 ± 5.0	43.2 ± 12.1
Statistical difference	$P < 0.001$	

Fig. 11. (A) SEM images of Ti implants (MAO treated at 270 V) removed from the tibia of rabbits 4 weeks after their implantation and (B) high magnification ($\times$ 500) micrograph of adhered chip.

4. Discussion

The purpose of this study was to improve the biocompatibility of Ti implants by modifying the composition and morphology of the implant surface. MAO is a simple, controllable, and cost-effective method of forming a porous TiO_2 layer on the implant surface. Moreover, MAO provides an ideal method of producing an oxide layer on the surface of implants which have a complex shape. The properties of the oxide layer, such as its thickness, microstructure, roughness, and concentrations of Ca and P are easily controllable by adjusting the voltage, current, processing time, and the concentration of the electrolyte during the MAO process [9,10,12,13].

The microstructural change of the oxide layer was found to be closely related to the voltage used for the MAO treatment. Increasing the voltage resulted in an increase in both the roughness and pore size, as well as in the thickness of the oxide layer (Figs. 1 and 2). These microstructural evolutions are attributed to the dielectric breakdown of the oxide layers [9,13]. During the MAO process, as the TiO_2 layer becomes thicker, micro-arc discharges occur on the local area of the substrate, that break down the surface dielectric layer to form micropores. At the same time, the oxide layer becomes thicker due to the increased extent of the electrochemical reaction as shown in Fig. 3. As the oxide layer becomes thicker, the resistance of the oxide layer increases and a higher potential energy is required to break down the dielectric layer. As a result of this series of reactions, the pore size and the roughness of the oxide layer increase rapidly.

The phase and composition changes were also closely related to the processes involved in the MAO treatment. At low voltage, only TiO_2 in the anatase phase was formed. With increasing MAO voltage, however, rutile TiO_2 was formed along with the anatase. Analogous behavior was observed during the thermal oxidation of Ti; at low temperature, anatase is formed, and at higher temperatures, the rutile phase becomes more stable than the anatase phase [1]. This oxidation behavior reflects the varying thermodynamic stability of TiO_2 depending on the treatment temperature. During the MAO process, the energy supplied to the system is proportional to the applied voltage. Therefore, the formation of rutile TiO_2 at higher voltage is a reasonable phenomenon. However, contrary to what happens in the case of thermal oxidation, the anatase which formed at the initial stage remained unchanged when the voltage was increased. The concentrations of Ca or P ions in the oxide layer are strongly dependent on the applied voltage. When the applied voltage was increased, more Ca or P ions present in the electrolyte were incorporated into the oxide layer.

The changes in chemical composition and roughness of the Ti surface played crucial roles in the biocompatibility of the implant. The proliferation rate was highest when the specimen was oxidized at the relatively low voltage of 190 V, and it decreased steadily with increasing voltage (Fig. 9). Even though there was some variation depending on the applied voltage, the number of cells increased more than 10 times compared to the originally plated cells. These proliferation results simply indicate that all of the specimens offered a biologically favorable environment. In contrast to the proliferation behavior, the ALP activity of the cells increased when the applied voltage was increased (Fig. 10). ALP activity is regarded as a marker for the early stages of cell differentiation. Generally, surface roughness affects cell proliferation and differentiation: increasing surface roughness decreases the cell proliferation rate, but increases ALP activity [20,21]. Moreover, cell differentiation is sensitive to chemical composition, but cell proliferation is not. Our result shows that the roughness and the amount of Ca and P ions incorporated into the titanium oxide layer strongly affect the cell response. Especially, the ALP activity significantly increased at higher voltages, which is deemed to be closely related to the increase in surface roughness and the increased amount of Ca and P contained in the oxide layer.

Preliminary in vivo tests on rabbits illustrated the effectiveness of MAO treatment in terms of the enhancement of the removal torque of the implanted specimens. The existence of titanium oxide on the Ti surface has been reported to improve bone formation [16,17,22]. Increase in surface roughness is also known to enhance the mechanical interlocking between the implant and the bones [23]. In this experiment, those specimens which were MAO treated at a voltage of 270 V were tested, because the specimens oxidized at higher voltages ($\geqslant 350$ V) had tiny cracks on the TiO_2 layer, as shown in Fig. 1(D). The removal torque of the MAO-treated Ti implants was more than three times higher than that of the as-machined Ti implant. This enhancement is attributable to the increase of surface roughness and to the presence of the Ca and P ions, which were incorporated into oxide layer during the MAO process. The existence of bone chips on the implant surface demonstrated the high bonding strength between the bone and the TiO_2 layer, as well as between the Ti substrate and the TiO_2 layer. More detailed and comprehensive biological evaluations of TiO_2 layers, with different physical and chemical characteristics, are in progress, and the results will be reported separately.

5. Conclusion

The MAO treatment of Ti, by bringing about positive physical and chemical changes to the Ti surface, had a beneficial effect on the biocompatibility of the Ti implant. Increasing the MAO voltage increased the thickness and roughness of the oxide layer, as well as the concentrations of Ca and P ions in the oxide layer. As a result of these changes, the ALP activity of the cells increased, while the cell proliferation rate decreased. The in vivo tests showed a considerable increase in removal torque (by a factor of 3) after the MAO treatment at 270 V compared to the as-machined pure titanium sample. Further studies involving in vivo histological observations, along with in vitro cellular calcification and mineralization assays are currently in progress.

Acknowledgements

References

[1] Brunette DM, Tengvall P, Textor M, Thomsen P. Titanium in medicine. Berlin: Springer; 2001.

[2] Boyan BD, Hummert TW, Dean DD, Schwartz Z. Role of material surfaces in regulating bone and cartilage cell response. Biomaterials 1996;17:137–46.

[3] Groessner-Schreiber B, Tuan RS. Enhanced extracellular matrix production and mineralization by osteoblasts cultured on titanium surfaces in vitro. J Cell Sci 1992;101:209–17.

[4] Larsson C, Thomsen P, Aronsson BO, Rodahl M, Lausmaa J, Kasemo B, Ericson LE. Bone response to surface-modified titanium implants: studies on the early tissue response to machined and electropolished implants with different oxide thicknesses. Biomaterials 1996;17:605–16.

[5] Hanawa T, Kamiura Y, Yamamoto S, Kohgo T, Amemiya A, Ukai H, Murakami K, Asaoka K. Early bone formation around calcium-ion-implanted titanium inserted into rat tibia. J Biomed Mater Res 1997;36:131–6.

[6] Li D, Ferguson SJ, Beutler T, Cochran DL, Sittig C, Hirt HP, Buser D. Biomechanical comparison of the sandblasted and acid-etched and the machined and acid-etched titanium surface for dental implants. J Biomed Mater Res 2002;60:325–32.

[7] de Groot K, Geesink R, Klein CPAT, Serekian P. Plasma-sprayed coatings of hydroxylapatite. J Biomed Mater Res 1987;21: 1375–81.

[8] Yerokhin AL, Nie X, Leyland A, Matthews A, Dowey SJ. Plasma electrolysis for surface engineering. Surf Coat Technol 1999;122:73–93.

[9] Ishizawa H, Ogino M. Formation and characterization of anodic titanium oxide films containing Ca and P. J Biomed Mater Res 1995;29:65–72.

[10] Ishizawa H, Ogino M. Characterization of thin hydroxyapatite layers formed on anodic titanium oxide films containing Ca and P by hydrothermal treatment. J Biomed Mater Res 1995;29: 1071–9.

[11] Ishizawa H, Fujino M, Ogino M. Histomorphometric evaluation of the thin hydroxyapatite layer formed through anodization followed by hydrothermal treatment. J Biomed Mater Res 1997;35:199–206.

[12] Sul YT, Johansson CB, Jeong Y, Albrektsson T. The electrochemical oxide growth behaviour on titanium in acid and alkaline electrolytes. Med Eng Phys 2001;23:329–46.

[13] Sul YT, Johansson CB, Petronis S, Krozer A, Jeong Y, Wennerberg A, Albrektsson T. Characteristics of the surface oxides on turned and electrochemically oxidized pure titanium implants up to dielectric breakdown: the oxide thickness, micropore configurations, surface roughness, crystal structure and chemical composition. Biomaterials 2002;23:491–501.

[14] Fini M, Cigada A, Rondelli G, Chiesa R, Giardino R, Giavaresi G, Aldini NN, Torricelli P, Vicentini B. In vitro and in vivo behaviour of Ca- and P-enriched anodized titanium. Biomaterials 1999;20:1587–94.

[15] Giavaresi G, Fini M, Cigada A, Chiesa R, Rondelli G, Rimondini L, Torricelli P, Toberto NN, Giardino R. Mechanical and histomorphometric evaluations of titanium implants with different surface treatments inserted in sheep cortical bone. Biomaterials 2003;24:1583–94.

[16] Sul YT, Johansson CB, Jeong Y, Röser K, Wennerberg A, Albrektsson T. Oxidized implants and their influence on the bone response. J Mater Sci Mater Med 2001;12:1025–31.

[17] Sul YT. The significance of the surface properties of oxidized titanium to the bone response: special emphasis on potential biochemical bonding of oxidized titanium implant. Biomaterials 2003;24:3893–907.

[18] Kim HW, Lee SY, Bae CJ, Noh YJ, Kim HE, Kim HM, Ko JS. Porous ZrO_2 bone scaffold coated with hydroxyapatite with fluorapatite intermediate layer. Biomaterials 2003;24:3277–84.

[19] Kim DH, Kong YM, Lee SH, Lee IS, Kim HE, Heo SJ, Koak JY. Composition and crystallization of hydroxyapatite coating layer

formed by electron beam deposition. J Am Ceram Soc 2003; 86:186–8.

[20] Martin JY, Schwartz Z, Hummert TW, Schraub DM, Simpson J, Lankford J, Dean DD, Cochran DL, Boyan BD. Effect of titanium surface roughness on proliferation, differentiation, and protein synthesis of human osteoblast-like cells (MG63). J Biomed Mater Res 1995;29:389–401.

[21] Boyan BD, Batzer R, Kieswetter K, Liu Y, Cochran DL, Szmuckler-Moncler S, Dean DD. Titanium surface roughness alters responsiveness of MG63 osteoblast-like cells to $1\alpha,25$-$(OH)_2D_3$. J Biomed Mater Res 1998;39:77–85.

[22] Thomsen P, Larsson C, Ericson LE, Sennerby L, Lausmaa J, Kasemo B. Structure of the interface between rabbit cortical bone and implants of gold, zirconium and titanium. J Mater Sci Mater Med 1997;8:653–65.

[23] Wennerberg A. The importance of surface roughness for implant incorporation. Int J Mach Tools Manuf 1998;38: 657–62.